# Supporting Information

## 1 Addendum to multipolar refinements

### 1.1 Resolution limit

Even though experimental reflections peaks are visible to a $\sin\theta/\lambda$ resolution of 2.07 Å$^{-1}$, it was necessary to introduce a cut-off in the high-order area owing to software limitations. A suitable cut-off was estimated by multipolar refinement employing the EHC model on noise-free static structure factors computed by W2k. The straightforward concept is that the EHC model will be able to describe the theoretical data down to a residual level of ±0.01 eÅ$^{-3}$ as long as no issues are present. The multipolar results for a systematic variation of the data resolution from 1.70 Å$^{-1}$ to 2.00 Å$^{-1}$ are displayed in Table 1. Significant residual features emerge at 1.80 Å$^{-1}$, and a further increase in the data resolution is followed by even stronger residual features. Thus, the upper limit for the theoretical data is positioned at 1.79 Å$^{-1}$. As to avoid potential influence from the radial screening parameters, the experimental limit was conservatively lowered to 1.70 Å$^{-1}$. Furthermore, it is noted that the multipole parameters are rather insensitive to the software limitations, Table 1.

**Table 1**

Multipolar refinement against static structure factors as function of data resolution. The EHC model is subject to constraints on $U_{\mathrm{iso}}$ and $s$.

| $\sin\theta/\lambda$ [Å$^{-1}$] | 1.70 | 1.79 | 1.80 | 1.90 | 2.00 |
|---|---|---|---|---|---|
| $\kappa_{\mathrm{v}}$ | 0.971 | 0.971 | 0.971 | 0.970 | 0.973 |
| $\kappa'_{\mathrm{v}}$ | 0.876 | 0.876 | 0.876 | 0.874 | 0.876 |
| *O2-* | 0.338 | 0.338 | 0.338 | 0.340 | 0.338 |
| *H0* | -0.105 | -0.106 | -0.106 | -0.108 | -0.102 |
| $P_{\mathrm{v}}$ | 4.014 | 4.014 | 4.014 | 4.012 | 4.016 |
| $\kappa_{\mathrm{c}}$ | 1.006 | 1.006 | 1.006 | 1.005 | 1.006 |
| $P_{\mathrm{c}}$ | 1.986 | 1.986 | 1.986 | 1.988 | 1.984 |
| $R_{\mathrm{F}}$ [%] | 0.01 | 0.01 | 0.01 | 0.01 | 0.03 |
| $\Delta\rho$ min/max [eÅ$^{-3}$] | -0.01/0.01 | -0.01/0.01 | -0.04/0.04 | -0.11/0.18 | -0.57/0.31 |

## 1.2 EHC/Rietveld extraction of $F_{\mathbf{obs}}$

The refinement model is upgraded from HC to EHC with the core parameters restricted to the experimentally determined values. Initially, this leads to an ADP increase from 0.001707(27) Å$^2$ to 0.001760(27) Å$^2$, Table 2. This alteration is in perfect quantitative concordance with reported refinement results based on SPring8 PXRD data (Fischer *et al.*, 2011). Attributable to correlation between the peak shape function and the ADP, it still remains essential to implement the iterative procedure of Wilson plot fitting. This converges rapidly to an ADP value of 0.001808(10) Å$^2$, Table 2. The resulting pattern fit attained by the simultaneous EHC/ Rietveld refinement is illustrated in Figure 1. As for the standard HC model, the success of this approach is corroborated by an increasing $U_{\mathrm{iso}}$ parameter accompanied by an improved structural accordance. This is highlighted by the agreement factors, $R_{\mathrm{F}}$ and $R_{\mathrm{wF}}$, and the residual density, $\Delta\rho\ \mathbf{r}$. The observant reader may notice that the final refinement displays an inferior residual fit compared to the HC case. This noteworthy difference originates from scaling errors. Contemplating the estimates derived from Wilson plot fitting, an increasing deviation from unity is observed, Table 2. The relative deviation of the converged estimate is -0.2 %, which is far larger than the corresponding term of the HC/Rietveld refinement, only deviating by 0.04 % from unity. Thus, this evidence further substantiates the need for separating the modeling of the PXRD pattern from the multipolar refinement when exploring subtle details in the electron density of diamond.

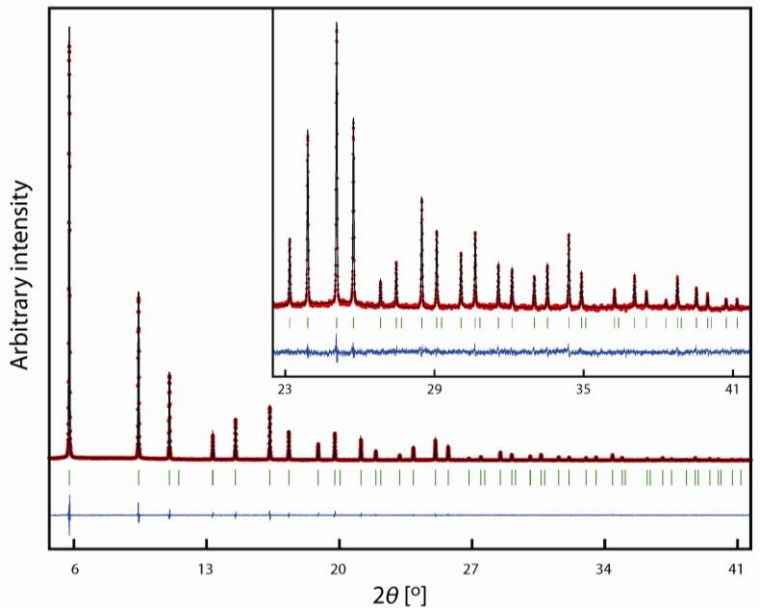


**Figure 1**
Converged EHC/Rietveld refinement with $U_{\mathrm{iso}}$ restricted to 0.001808 Å$^2$. Observed (red circles), calculated (black) and difference pattern (blue).

## Table 2

Parameter overview for the iterative series of simultaneous EHC/Rietveld refinements. Each refinement is characterized by weighted and non-weighted agreement factors for the pattern fit ($R_{\mathrm{P}}$, $R_{\mathrm{wP}}$) and for the structural fit ($R_{\mathrm{F}}$, $R_{\mathrm{wF}}$). $U_{\mathrm{iso}}$ W and $s$ W are the estimates deduced from Wilson plot fitting; coefficient of determination was 0.998 for all linear least-square fits. Fixed values have a superscript of $^{\mathrm{F}}$.

| cycle | 1 | 2 | 3 | 4 |
|---|---|---|---|---|
| $U_{\mathrm{iso}}$ [Å$^2$] | 0.001760(27) | 0.001799$^{\mathrm{F}}$ | 0.001806$^{\mathrm{F}}$ | 0.001808$^{\mathrm{F}}$ |
| $a$ [Å] | 3.566606(6) | 3.566606(6) | 3.566606(6) | 3.566606(6) |
| *zero shift* | -0.030(2) | -0.030(2) | -0.030(2) | -0.030(2) |
| *scale* | 2.619(4) | 2.625(2) | 2.626(2) | 2.626(2) |
| *GU* | 9.3(5) | 9.1(4) | 9.1(4) | 9.1(4) |
| *GW* | 2.59(1) | 2.59(1) | 2.59(1) | 2.59(1) |
| *LX* | 0.907(7) | 0.907(7) | 0.907(7) | 0.907(7) |
| $\kappa_{\mathrm{v}}$ | 0.962(4) | 0.958(3) | 0.958(3) | 0.958(3) |
| $\kappa'_{\mathrm{v}}$ | 0.86(1) | 0.86(1) | 0.86(1) | 0.86(1) |
| *O2-* | 0.36(1) | 0.362(9) | 0.362(9) | 0.36(1) |
| *H0* | -0.16(2) | -0.17(2) | -0.17(2) | -0.17(2) |
| $R_{\mathrm{F}}$ | 0.45 | 0.36 | 0.35 | 0.35 |
| $R_{\mathrm{wF}}$ | 0.61 | 0.46 | 0.44 | 0.44 |
| $R_{\mathrm{P}}$ | 1.76 | 1.76 | 1.76 | 1.76 |
| $R_{\mathrm{wP}}$ | 2.64 | 2.64 | 2.64 | 2.64 |
| $\chi^2$ | 3.27 | 3.27 | 3.27 | 3.27 |
| $\Delta\rho$ min/max [eÅ$^{-3}$] | -0.53/0.12 | -0.31/0.12 | -0.27/0.12 | -0.26/0.12 |
| $U_{\mathrm{iso}}$ W [Å$^2$] | 0.001799(10) | 0.001806(10) | 0.001808(10) | 0.001808(10) |
| $s$ W | 0.9998(13) | 0.9981(13) | 0.9978(13) | 0.9978(13) |

## 1.3 Static residual density

In order to promote the correspondence between theory and experiment, we have for the HC/Rietveld and EHC/Rietveld extracted $F_{\mathrm{obs}}$ calculated static residual densities, Figure 2. The thermal motion was deconvoluted by simple multiplication based on their Wilson plot derived ADP. The static residual plots exhibit more distinct features, among which the most notably is the increased positive density on the carbon site. The direction of the alterations follows the predictions outlined by the theoretical W2k computation.

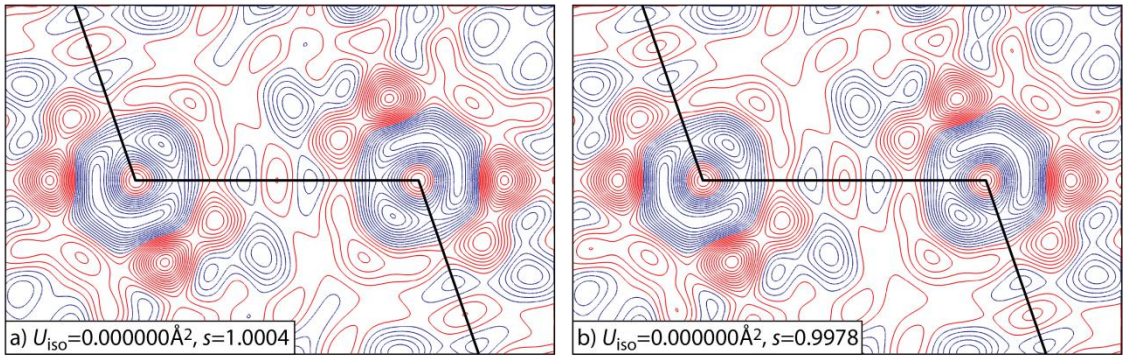


**Figure 2**

Static residual density maps in the (110) plane of the diamond lattice shown for HC multipolar refinement based on (*a*) the $F_{\mathrm{obs}}$ extracted using the HC model and (*b*) the $F_{\mathrm{obs}}$ extracted using the EHC model. $U_{\mathrm{iso}}$ is fixed at zero and $s$ is constrained to the estimate derived from Wilson plot fitting. Positive (red) and negative (blue) contour lines are drawn employing a step width of 0.01 eÅ$^{-3}$ and including all structure factors to a $\sin\theta/\lambda$ resolution of 1.70 Å$^{-1}$. The black line represents the C-C bonding chain.

## 1.4 Structure factors

| HC/Rietveld extracted $F_{obs}$ | | | | | | | | | |
|---|---|---|---|---|---|---|---|---|---|
| $h$ | $k$ | $l$ | $F_{obs}$ | $\sigma_{obs}$ | $h$ | $k$ | $l$ | $F_{obs}$ | $\sigma_{obs}$ |
| 1 | 1 | 1 | 18.574 | 0.186 | 1 | 1 | 9 | 3.713 | 0.039 |
| 2 | 0 | 2 | 15.404 | 0.154 | 6 | 4 | 6 | 4.955 | 0.057 |
| 1 | 1 | 3 | 9.225 | 0.092 | 3 | 1 | 9 | 3.371 | 0.040 |
| 2 | 2 | 2 | 0.884 | 0.054 | 4 | 4 | 8 | 4.557 | 0.056 |
| 0 | 0 | 4 | 11.860 | 0.120 | 7 | 1 | 7 | 3.107 | 0.035 |
| 3 | 1 | 3 | 8.380 | 0.084 | 3 | 3 | 9 | 3.107 | 0.035 |
| 2 | 2 | 4 | 10.785 | 0.108 | 5 | 5 | 7 | 3.104 | 0.035 |
| 3 | 3 | 3 | 7.200 | 0.072 | 6 | 2 | 8 | 4.160 | 0.044 |
| 1 | 1 | 5 | 7.261 | 0.073 | 2 | 0 | 10 | 4.159 | 0.044 |
| 4 | 0 | 4 | 9.659 | 0.098 | 7 | 3 | 7 | 2.878 | 0.035 |
| 3 | 1 | 5 | 6.540 | 0.066 | 5 | 1 | 9 | 2.879 | 0.035 |
| 2 | 0 | 6 | 8.688 | 0.088 | 5 | 3 | 9 | 2.599 | 0.041 |
| 3 | 3 | 5 | 5.968 | 0.061 | 4 | 2 | 10 | 3.520 | 0.044 |
| 4 | 4 | 4 | 7.870 | 0.084 | 7 | 5 | 7 | 2.428 | 0.043 |
| 1 | 1 | 7 | 5.377 | 0.055 | 1 | 1 | 11 | 2.426 | 0.043 |
| 5 | 1 | 5 | 5.398 | 0.055 | 8 | 0 | 8 | 3.260 | 0.113 |
| 4 | 2 | 6 | 7.195 | 0.073 | 7 | 1 | 9 | 2.251 | 0.029 |
| 3 | 1 | 7 | 4.898 | 0.050 | 3 | 1 | 11 | 2.251 | 0.029 |
| 5 | 3 | 5 | 4.887 | 0.050 | 5 | 5 | 9 | 2.252 | 0.029 |
| 0 | 0 | 8 | 6.449 | 0.087 | 6 | 6 | 8 | 2.998 | 0.045 |
| 3 | 3 | 7 | 4.438 | 0.050 | 6 | 0 | 10 | 2.998 | 0.045 |
| 6 | 0 | 6 | 5.913 | 0.061 | 7 | 3 | 9 | 2.051 | 0.038 |
| 2 | 2 | 8 | 5.910 | 0.061 | 3 | 3 | 11 | 2.050 | 0.038 |
| 5 | 5 | 5 | 4.069 | 0.043 | 8 | 4 | 8 | 2.781 | 0.064 |
| 5 | 1 | 7 | 4.059 | 0.043 | 0 | 0 | 12 | 2.780 | 0.064 |
| 4 | 0 | 8 | 5.390 | 0.059 | 7 | 7 | 7 | 1.896 | 0.050 |
| 5 | 3 | 7 | 3.719 | 0.039 | 5 | 1 | 11 | 1.896 | 0.050 |

| EHC /Rietveld extracted $F_{\mathrm{obs}}$ | | | | | | | | | |
|---|---|---|---|---|---|---|---|---|---|
| $h$ | $k$ | $l$ | $F_{\mathrm{obs}}$ | $\sigma_{\mathrm{obs}}$ | $h$ | $k$ | $l$ | $F_{\mathrm{obs}}$ | $\sigma_{\mathrm{obs}}$ |
| 1 | 1 | 1 | 18.534 | 0.185 | 1 | 1 | 9 | 3.708 | 0.039 |
| 2 | 0 | 2 | 15.371 | 0.154 | 6 | 4 | 6 | 4.950 | 0.057 |
| 1 | 1 | 3 | 9.205 | 0.092 | 3 | 1 | 9 | 3.368 | 0.039 |
| 2 | 2 | 2 | 0.888 | 0.053 | 4 | 4 | 8 | 4.554 | 0.056 |
| 0 | 0 | 4 | 11.835 | 0.119 | 7 | 1 | 7 | 3.104 | 0.035 |
| 3 | 1 | 3 | 8.362 | 0.084 | 3 | 3 | 9 | 3.104 | 0.035 |
| 2 | 2 | 4 | 10.762 | 0.108 | 5 | 5 | 7 | 3.101 | 0.035 |
| 3 | 3 | 3 | 7.177 | 0.072 | 6 | 2 | 8 | 4.156 | 0.044 |
| 1 | 1 | 5 | 7.249 | 0.073 | 2 | 0 | 10 | 4.154 | 0.044 |
| 4 | 0 | 4 | 9.640 | 0.098 | 7 | 3 | 7 | 2.875 | 0.034 |
| 3 | 1 | 5 | 6.527 | 0.066 | 5 | 1 | 9 | 2.877 | 0.034 |
| 2 | 0 | 6 | 8.671 | 0.087 | 5 | 3 | 9 | 2.599 | 0.041 |
| 3 | 3 | 5 | 5.957 | 0.061 | 4 | 2 | 10 | 3.517 | 0.043 |
| 4 | 4 | 4 | 7.857 | 0.084 | 7 | 5 | 7 | 2.427 | 0.043 |
| 1 | 1 | 7 | 5.367 | 0.055 | 1 | 1 | 11 | 2.426 | 0.043 |
| 5 | 1 | 5 | 5.388 | 0.055 | 8 | 0 | 8 | 3.266 | 0.112 |
| 4 | 2 | 6 | 7.181 | 0.072 | 7 | 1 | 9 | 2.250 | 0.029 |
| 3 | 1 | 7 | 4.890 | 0.050 | 3 | 1 | 11 | 2.250 | 0.029 |
| 5 | 3 | 5 | 4.878 | 0.050 | 5 | 5 | 9 | 2.251 | 0.029 |
| 0 | 0 | 8 | 6.442 | 0.087 | 6 | 6 | 8 | 2.998 | 0.044 |
| 3 | 3 | 7 | 4.432 | 0.050 | 6 | 0 | 10 | 2.998 | 0.044 |
| 6 | 0 | 6 | 5.904 | 0.061 | 7 | 3 | 9 | 2.053 | 0.038 |
| 2 | 2 | 8 | 5.901 | 0.061 | 3 | 3 | 11 | 2.052 | 0.038 |
| 5 | 5 | 5 | 4.064 | 0.043 | 8 | 4 | 8 | 2.782 | 0.063 |
| 5 | 1 | 7 | 4.053 | 0.043 | 0 | 0 | 12 | 2.781 | 0.063 |
| 4 | 0 | 8 | 5.383 | 0.059 | 7 | 7 | 7 | 1.897 | 0.050 |
| 5 | 3 | 7 | 3.714 | 0.039 | 5 | 1 | 11 | 1.898 | 0.050 |

**Static structure factors computed by *Wien2k***

| $h$ | $k$ | $l$ | $F_{\mathrm{W2k}}$ | $h$ | $k$ | $l$ | $F_{\mathrm{W2k}}$ |
|---|---|---|---|---|---|---|---|
| 1 | 1 | 1 | 18.610 | 5 | 7 | 7 | 3.434 |
| 0 | 2 | 2 | 15.783 | 7 | 7 | 7 | 2.910 |
| 2 | 2 | 2 | 0.907 | 0 | 0 | 8 | 7.779 |
| 1 | 1 | 3 | 9.595 | 2 | 2 | 8 | 7.252 |
| 1 | 3 | 3 | 8.827 | 0 | 4 | 8 | 6.773 |
| 3 | 3 | 3 | 7.752 | 2 | 4 | 8 | 0.004 |
| 0 | 0 | 4 | 12.517 | 4 | 4 | 8 | 5.943 |
| 2 | 2 | 4 | 11.510 | 2 | 6 | 8 | 5.584 |
| 0 | 4 | 4 | 10.583 | 4 | 6 | 8 | 0.004 |
| 2 | 4 | 4 | 0.072 | 6 | 6 | 8 | 4.432 |
| 4 | 4 | 4 | 9.035 | 0 | 8 | 8 | 4.683 |
| 1 | 1 | 5 | 7.862 | 2 | 8 | 8 | 0.001 |
| 1 | 3 | 5 | 7.225 | 4 | 8 | 8 | 4.200 |
| 3 | 3 | 5 | 6.738 | 1 | 1 | 9 | 4.669 |
| 1 | 5 | 5 | 6.217 | 1 | 3 | 9 | 4.373 |
| 3 | 5 | 5 | 5.747 | 3 | 3 | 9 | 4.106 |
| 5 | 5 | 5 | 5.009 | 1 | 5 | 9 | 3.860 |
| 0 | 2 | 6 | 9.744 | 3 | 5 | 9 | 3.634 |
| 2 | 2 | 6 | 0.024 | 5 | 5 | 9 | 3.245 |
| 2 | 4 | 6 | 8.377 | 1 | 7 | 9 | 3.242 |
| 4 | 4 | 6 | 0.017 | 3 | 7 | 9 | 3.072 |
| 0 | 6 | 6 | 7.255 | 0 | 2 | 10 | 5.583 |
| 2 | 6 | 6 | 0.007 | 2 | 2 | 10 | 0.001 |
| 4 | 6 | 6 | 6.338 | 2 | 4 | 10 | 4.957 |
| 6 | 6 | 6 | 0.006 | 4 | 4 | 10 | 0.002 |
| 1 | 1 | 7 | 6.196 | 0 | 6 | 10 | 4.431 |
| 1 | 3 | 7 | 5.764 | 2 | 6 | 10 | 0.001 |
| 3 | 3 | 7 | 5.351 | 1 | 1 | 11 | 3.430 |
| 1 | 5 | 7 | 4.996 | 1 | 3 | 11 | 3.243 |
| 3 | 5 | 7 | 4.676 | 3 | 3 | 11 | 3.070 |
| 5 | 5 | 7 | 4.100 | 1 | 5 | 11 | 2.911 |
| 1 | 7 | 7 | 4.106 | 0 | 0 | 12 | 4.199 |
| 3 | 7 | 7 | 3.857 | | | | |